Mon. Not. R. Astron. Soc. **000**, 1–11 (2009) Printed 12 October 2009 (MN LATEX style file v2.2)

The progenitors of Type Ia supernovae with long delay times

Bo Wang,[1,3⋆] Xiang-Dong Li[2] and Zhan-Wen Han[1]
[1] *National Astronomical Observatories/Yunnan Observatory, the Chinese Academy of Sciences, Kunming 650011, China*
[2] *Department of Astronomy, Nanjing University, Nanjing 210093, China*
[3] *Graduate University of Chinese Academy of Sciences, Beijing 100049, China*

12 October 2009

ABSTRACT

The nature of the progenitors of Type Ia supernovae (SNe Ia) is still unclear. In this paper, by considering the effect of the instability of accretion disk on the evolution of white dwarf (WD) binaries, we performed binary evolution calculations for about 2400 close WD binaries, in which a carbon–oxygen WD accretes material from a main-sequence star or a slightly evolved subgiant star (WD + MS channel), or a red-giant star (WD + RG channel) to increase its mass to the Chandrasekhar (Ch) mass limit. According to these calculations, we mapped out the initial parameters for SNe Ia in the orbital period–secondary mass ($\log P^{\rm i} - M_2^{\rm i}$) plane for various WD masses for these two channels, respectively. We confirm that WDs in the WD + MS channel with a mass as low as $0.61\,M_\odot$ can accrete efficiently and reach the Ch limit, while the lowest WD mass for the WD + RG channel is $1.0\,{\rm M}_\odot$. We have implemented these results in a binary population synthesis study to obtain the SN Ia birthrates and the evolution of SN Ia birthrates with time for both a constant star formation rate and a single starburst. We find that the Galactic SN Ia birthrate from the WD + MS channel is $\sim 1.8\times10^{-3}$ yr^{-1} according to our standard model, which is higher than previous results. However, similar to previous studies, the birthrate from the WD + RG channel is still low ($\sim 3\times10^{-5}$ yr^{-1}). We also find that about one third of SNe Ia from the WD + MS channel and all SNe Ia from the WD + RG channel can contribute to the old populations ($\gtrsim$1 Gyr) of SN Ia progenitors.

Key words: binaries: close – stars: evolution – white dwarfs – supernovae: general

1 INTRODUCTION

Type Ia supernovae (SNe Ia) play an important role in astrophysics, especially in cosmology. They appear to be good cosmological distance indicators and have been applied successfully to the task of determining cosmological parameters (e.g. Ω and Λ: Riess et al. 1998; Perlmutter et al. 1999). They are also a key part of our understanding of galactic chemical evolution owing to the main contribution of iron to their host galaxies (e.g. Greggio & Renzini 1983; Matteucci & Greggio 1986). Despite their importance, several key issues related to the nature of their progenitors and the physics of the explosion mechanisms are still not well understood (Hillebrandt & Niemeyer 2000; Röpke & Hillebrandt 2005; Podsiadlowski et al. 2008; Wang et al. 2008a), and no SN Ia progenitor system has been conclusively identified pre-explosion.

There is a broad agreement that SNe Ia are thermonuclear explosions of carbon–oxygen white dwarfs (CO WDs) in binaries (see the review of Nomoto, Iwamoto & Kishimoto 1997). Over the last few decades, two competing progenitor models of SNe Ia were discussed frequently, i.e. the double-degenerate (DD) and single-degenerate (SD) models. Of these two models, the SD model (Whelan & Iben 1973; Nomoto, Thielemann & Yokoi 1984; Fedorova, Tutukov & Yungelson 2004; Han 2008) is widely accepted at present. It is suggested that the DD model, which involves the merger of two CO WDs (Iben & Tutukov 1984; Webbink 1984; Han 1998), likely leads to an accretion-induced collapse rather than a SN Ia (Nomoto & Iben 1985; Saio & Nomoto 1985; Timmes, Woosley & Taam 1994). For the SD model, the companion is probably a main-sequence (MS) star or a slightly evolved subgiant star (WD + MS channel), or a red-giant star (WD + RG channel), or even a He star (WD + He star channel) (Hachisu, Kato & Nomoto 1996; Li & van den Heuvel 1997; Hachisu et al. 1999a; Langer et al. 2000; Han & Podsiadlowski 2004, 2006; Wang et al. 2009a,b). Although the SD model is currently a favorable progenitor

⋆ E-mail: wangbo@ynao.ac.cn

model of SNe Ia, any single channel of the model cannot account for the birthrate inferred observationally. Note that, some recent observations have indirectly suggested that at least some SNe Ia can be produced by a variety of different progenitor systems (e.g. Hansen 2003; Ruiz-Lapuente et al. 2004; Patat et al. 2007; Voss & Nelemans 2008; Wang et al. 2008b; Justham et al. 2009).

At present, various progenitor models of SNe Ia can be examined by comparing the distribution of the delay time (between the star formation and SN Ia explosion) expected from a progenitor channel with that of observations (e.g. Chen & Li 2007; Meng, Chen & Han 2009; Lü et al. 2009; Ruiter, Belczynski & Fryer 2009). Mannucci, Della Valle & Panagia (2006) argued for the existence of two separate SN Ia populations, a 'prompt' component with a delay time less than ∼100 Myr, and a 'delayed' component with a delay time ∼3 Gyr. By investigating the star formation history (SFH) of 257 SN Ia host galaxies, Aubourg et al. (2008) found evidence of a short-lived population of SN Ia progenitors with lifetimes less than 180 Myr. Botticella et al. (2008) and Totani et al. (2008) analyzed host galaxies of SNe Ia and concluded that a substantial fraction of SNe Ia must have long delay times on the order of 2−3 Gyr. Moreover, Schawinski (2009) recently constrained the minimum delay time of 21 nearby SNe Ia by investigating their host galaxies (early-type galaxies). The study showed that these early-type host galaxies lack 'prompt' SNe Ia with a delay time less than ∼100 Myr and that ∼70 per cent SNe Ia have minimum delay times of 275 Myr−1.25 Gyr, while at least 20 per cent SNe Ia have minimum delay times of at least 1 Gyr at 95 per cent confidence and two of these four SNe Ia are likely older than 2 Gyr.

For SNe Ia with the short delay times, Wang et al. (2009a) studied a WD + He star channel to produce SNe Ia, in which a CO WD accretes material from a He MS star or a He subgiant to increase its mass to the Chandrasekhar (Ch) mass. The study showed the parameter spaces for the progenitors of SNe Ia. By using a detailed binary population synthesis (BPS) approach, Wang et al. (2009b, WCMH09) found that the Galactic SN Ia birthrate from this channel is $\sim 0.3 \times 10^{-3}$ yr^{-1}, and that this channel can produce SNe Ia with short delay times (∼45−140 Myr). For SNe Ia with the long delay times ($\gtrsim$1 Gyr), this requires that the mass of the companion should be $\lesssim 2\,M_\odot$.

Recently, Xu & Li (2009) emphasized that the mass-transfer through the Roche lobe overflow (RLOF) in the evolution of WD binaries may become unstable (at least during part of the mass-transfer lifetime), i.e. the mass-transfer rate is not equivalent to the mass-accretion rate onto the WD. This important feature has been ignored in nearly all of the previous theoretical works on SN Ia progenitors except for King, Rolfe & Schenker (2003) [1] and Xu & Li (2009), who inferred that the mass-accretion rate onto the WD during dwarf nova outbursts can be sufficiently high to allow steady nuclear burning of the accreted matter and growth of the WD mass. In particular, the study of Xu & Li (2009) enlarges the region of SN Ia parameter spaces. However, they only give the SN Ia parameter spaces with WD initial masses of 0.8 and 1 $M_\odot$. More detailed work is obviously needed to investigate the influence of the accretion disk on the final results and to give SN Ia birthrates and delay times.

Including the effect of the instability of accretion disk on the evolution of WD binaries, the purpose of this paper is to study the WD + MS and WD + RG channels towards SNe Ia comprehensively and systematically, and then to determine the parameter spaces for SNe Ia, which can be used in BPS studies. In Section 2, we describe the numerical code for the binary evolution calculations and the grid of the binary models. The binary evolutionary results are shown in Section 3. We describe the BPS method in Section 4 and present the BPS results in section 5. Finally, a discussion is given in Section 6, and a summary in Section 7.

2 BINARY EVOLUTION CALCULATIONS

In our WD binary models, the lobe-filling star is a MS star or a subgiant star (WD + MS channel), or a red-giant star (WD + RG channel). The star transfers some of its material onto the surface of the WD, which increases the mass of the WD as a consequence. If the WD grows to 1.378 $M_\odot$, we assume that it explodes as a SN Ia.

2.1 Stellar evolution code

We use Eggleton's stellar evolution code (Eggleton 1971, 1972, 1973) to calculate the WD binary evolutions. The code has been updated with the latest input physics over the last three decades (Han, Podsiadlowski & Eggleton 1994; Pols et al. 1995, 1998). RLOF is treated within the code described by Han, Tout & Eggleton (2000). We set the ratio of mixing length to local pressure scale height, $\alpha = l/H_{\rm p}$, to be 2.0 and set the convective overshooting parameter, $\delta_{\rm OV}$, to be 0.12 (Pols et al. 1997; Schröder, Pols & Eggleton 1997), which roughly corresponds to an overshooting length of ∼0.25 pressure scaleheights ($H_{\rm P}$). The opacity tables are compiled by Chen & Tout (2007) from Iglesias & Rogers (1996) and Alexander & Ferguson (1994). In our calculations we use a typical Pop I composition with H abundance $X = 0.70$, He abundance $Y = 0.28$ and metallicity $Z = 0.02$.

2.2 Mass-accretion rates

During the mass-transfer through the RLOF, the accreting material can form an accretion disk surrounding the WD, which may become thermally unstable when the effective temperature in the disk falls below the H ionization temperature ∼6500 K (e.g. van Paradijs 1996; King et al. 1997; Lasota 2001). This also corresponds to a critical mass-transfer rate below which the disk is unstable. Similar to the work of Xu & Li (2009), we also set the critical mass-transfer rate for a stable accretion disk to be

$$\dot{M}_{\rm cr,disk} \simeq 4.3 \times 10^{-9}\,(P_{\rm orb}/4\,{\rm hr})^{1.7}\,{\rm M}_\odot\,{\rm yr}^{-1}, \quad (1)$$

for WD accretors (van Paradijs 1996), where $P_{\rm orb}$ is the orbital period. The locations of various types of cataclysmic variable stars (e.g. the UX UMa, U Gem, SU UMa, and

[1] King, Rolfe & Schenker (2003) adopted a similar method in Li & Wang (1998) to produce SNe Ia with long period dwarf novae in a semi-analytic approach.

Z Cam systems) in a ($P_{\rm orb}$, $\dot{M}_{\rm cr,disk}$) diagram are well described by this expression (Smak 1983; Osaki 1996; van Paradijs 1996).

If the mass-transfer rate, $|\dot{M}_2|$, is higher than the critical value $\dot{M}_{\rm cr,disk}$, we assume that the accretion disk is stable and the WD accretes smoothly at a rate $\dot{M}_{\rm acc} = |\dot{M}_2|$; otherwise the WD accretes only during outbursts and the mass-accretion rate is $\dot{M}_{\rm acc} = |\dot{M}_2|/d$, where d is the duty cycle. The mass-accretion rate is $\dot{M}_{\rm acc} = 0$ during quiescence. King, Rolfe & Schenker (2003) showed that for typical values of the duty cycle $\sim$0.1 to a few 10^{-3} the accretion rates onto the WD during dwarf nova outbursts can be sufficiently high to allow steady nuclear burning of the accreted matter. The limits on the duty cycles of dwarf nova outbursts come from observations (Warner 1995): (1) The outburst intervals for each object are quasi-periodic, but within the dwarf nova family, the intervals can range from days to decades. (2) The lifetime of an outburst is typically from 2 to 20 days and is correlated with the outburst interval. The quasi-periodicity of the dwarf nova outbursts allows to use a single duty cycle to roughly describe the change in the mass-transfer rate, though we note that this is a simplification of the real, complicated processes. In this paper we set the duty cycle to be 0.01 (we will discuss the effects of varying the assumed value in the discussion section).

2.3 Mass-growth rates

Instead of solving stellar structure equations of a WD, we adopt the prescription of Hachisu et al. (1999a) for the mass-growth of a CO WD by accretion of H-rich material from its companion. The prescription is given below. If the mass-accretion rate of the WD, $\dot{M}_{\rm acc}$, is above a critical rate, $\dot{M}_{\rm cr,WD}$, we assume that the accreted H steadily burns on the surface of the WD and that the H-rich material is converted into He at a rate $\dot{M}_{\rm cr,WD}$. The unprocessed matter is assumed to be lost from the system as an optically thick wind at a mass-loss rate $\dot{M}_{\rm wind} = |\dot{M}_2| - \dot{M}_{\rm cr,WD}$. The critical mass-accretion rate is

$$\dot{M}_{\rm cr,WD} = 5.3{\times}10^{-7}\,\frac{(1.7-X)}{X}(M_{\rm WD}/M_\odot{-}0.4)\,M_\odot\,yr^{-1}, \quad (2)$$

where X is the H mass fraction and $M_{\rm WD}$ is the mass of the accreting WD.

The following assumptions are adopted when $|\dot{M}_{\rm acc}|$ is smaller than $\dot{M}_{\rm cr,WD}$.

(1) When $|\dot{M}_{\rm acc}|$ is less than $\dot{M}_{\rm cr,WD}$ but higher than $\frac{1}{2}\dot{M}_{\rm cr,WD}$, the H-shell burning is steady and no mass is lost from the system.

(2) When $|\dot{M}_{\rm acc}|$ is lower than $\frac{1}{2}\dot{M}_{\rm cr,WD}$ but higher than $\frac{1}{8}\dot{M}_{\rm cr,WD}$, a very weak H-shell flash is triggered but no mass is lost from the system.

(3) When $|\dot{M}_{\rm acc}|$ is lower than $\frac{1}{8}\dot{M}_{\rm cr,WD}$, the H-shell flash is so strong that no material is accumulated onto the surface of the WD.

We define the mass-growth rate of the He layer under the H-shell burning as

$$\dot{M}_{\rm He} = \eta_{\rm H}|\dot{M}_{\rm acc}|, \quad (3)$$

where $\eta_{\rm H}$ is the mass-accumulation efficiency for H-shell burning. According to the assumptions above, the values of $\eta_{\rm H}$ are:

$$\eta_{\rm H} = \begin{cases} \dot{M}_{\rm cr,WD}/|\dot{M}_{\rm acc}|, & |\dot{M}_{\rm acc}| > \dot{M}_{\rm cr,WD}, \\ 1, & \dot{M}_{\rm cr,WD} \geqslant |\dot{M}_{\rm acc}| \geqslant \frac{1}{8}\dot{M}_{\rm cr,WD}, \\ 0, & |\dot{M}_{\rm acc}| < \frac{1}{8}\dot{M}_{\rm cr,WD}. \end{cases} \quad (4)$$

When the mass of the He layer reaches a certain value, He is assumed to be ignited. If He-shell flashes occur, a part of the envelope mass is assumed to be blown off. The mass-growth rate of WDs in this case is linearly interpolated from a grid computed by Kate & Hachisu (2004), where a wide range of WD mass and mass-accretion rate were calculated in the He-shell flashes.

We define the mass-growth rate of the CO WD, $\dot{M}_{\rm CO}$, as

$$\dot{M}_{\rm CO} = \eta_{\rm He}\dot{M}_{\rm He} = \eta_{\rm He}\eta_{\rm H}|\dot{M}_{\rm acc}|, \quad (5)$$

where $\eta_{\rm He}$ is the mass-accumulation efficiency for He-shell flashes.

2.4 Orbital angular momentum losses

The evolution of these WD binaries is driven by the nuclear evolution of the donor stars, and the change of the orbital angular momentum of the binaries is mainly caused by wind mass-loss from the WD. We assume that the mass lost from these binaries carries away the same specific orbital angular momentum of the WD (the mass-loss in the donor's wind is supposed to be negligible, but its effect on the change of the orbital angular momentum, i.e. magnetic braking, is included, e.g. Li & van den Heuvel 1997).

For the magnetic braking (MB) effect, we adopt the description of angular momentum loss from Sills, Pinsonneault & Terndrup (2000),

$$\frac{{\rm d}J_{\rm MB}}{{\rm d}t} = \begin{cases} -K\omega^3\left(\frac{R_2}{R_\odot}\right)^{0.5}\left(\frac{M_2}{M_\odot}\right)^{-0.5}, & \omega \leqslant \omega_{\rm crit}, \\ -K\omega_{\rm crit}^2\omega\left(\frac{R_2}{R_\odot}\right)^{0.5}\left(\frac{M_2}{M_\odot}\right)^{-0.5}, & \omega > \omega_{\rm crit}, \end{cases} \quad (6)$$

where $K = 2.7\times10^{47}$ g cm^2 s (Andronov, Pinsonneault & Sills 2003), ω is the angular velocity of the binary, and $\omega_{\rm crit}$ is the critical angular velocity at which the angular momentum loss rate reaches a saturated state (Krishnamurthi et al. 1997). Following the suggestion of Podsiadlowski, Rappaport & Pfahl (2002), we also add an ad hoc factor $\exp(-0.02/q_{\rm conv}+1)$ if $q_{\rm conv} < 0.02$ in Equation (6), where $q_{\rm conv}$ is the mass fraction of the surface convective envelop, to reduce the MB effect when the convective envelope becomes too small.

2.5 Grid calculations

We incorporate the prescriptions above into Eggleton's stellar evolution code and follow the evolution of WD + MS systems. We have calculated about 2400 WD + MS systems, and obtained a large, dense model grid, in which the lobe-filling star is a MS star or a subgiant star (WD + MS channel), or a RG star (WD + RG channel). The initial mass of the donor star, $M_2^{\rm i}$, ranges from 0.5$-$4.0 $M_\odot$; the initial mass of the CO WD, $M_{\rm WD}^{\rm i}$, is from 0.61$-$1.20 $M_\odot$; the initial orbital period of the binary system, $P^{\rm i}$, changes from the minimum value, at which a zero-age MS (ZAMS) star would fill its Roche lobe, to $\sim$40 d.

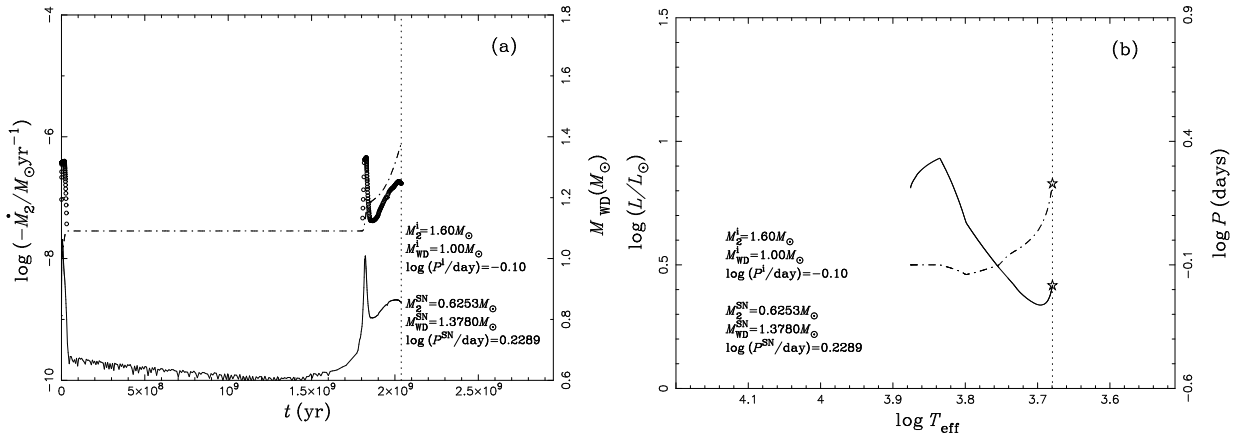

Figure 1. An example of binary evolution calculations. In panel (a), the solid and dash-dotted curves show $\dot{M}_2$ and $M_{\rm WD}$ varing with time, respectively. The open circles represent the evolution of $\dot{M}_{\rm CO}$ during outbursts. In panel (b), the evolutionary track of the donor star is shown as a solid curve and the evolution of orbital period is shown as a dash-dotted curve. Dotted vertical lines in both panels and asterisks in panel (b) indicate the position where the WD is expected to explode as a SN Ia. The initial binary parameters and the parameters at the moment of the SN Ia explosion are also given in these two panels.

3 BINARY EVOLUTION RESULTS

3.1 An example of binary evolution calculations

In Fig. 1, we present an example of binary evolution calculations. Panel (a) shows the $\dot{M}_2$, $\dot{M}_{\rm CO}$ and $M_{\rm WD}$ varing with time, while panel (b) is the evolutionary track of the donor star in the Hertzsprung-Russell diagram, where the evolution of the orbital period is also shown. The binary shown in this case is ($M_2^{\rm i}$, $M_{\rm WD}^{\rm i}$, $\log(P^{\rm i}/{\rm day})$) = (1.6, 1.0, −0.1), where $M_2^{\rm i}$, $M_{\rm WD}^{\rm i}$ and $P^{\rm i}$ are the initial mass of the donor star and the CO WD in solar masses, and the initial orbital period in days, respectively. The donor star fills its Roche lobe on the MS which results in case A mass-transfer. During the whole evolution, the mass-transfer rate is lower than the critical value given by Equation (1). Thus, the accretion disk experiences instability. The mass-accretion rate $\dot{M}_{\rm acc}$ of the WD exceeds $\frac{1}{8}\dot{M}_{\rm cr,WD}$ after the onset of RLOF, leading to the mass-growth of the WD. With the continuous decreasing of $|\dot{M}_2|$, when $\dot{M}_{\rm acc}$ drops below $\frac{1}{8}\dot{M}_{\rm cr,WD}$ after about 5×10^7 yr, the H-shell flash is so strong that no material is accumulated onto the surface of the WD. At about 1.7×10^9 yr, $|\dot{M}_2|$ increases again as the donor star evolves off the MS and expands, allowing the mass-growth of the WD during outbursts. When the WD grows to 1.378 $M_\odot$, it explodes as a SN Ia. At the SN explosion moment, the mass of the donor star is $M_2^{\rm SN} = 0.6253\,M_\odot$ and the orbital period $\log(P^{\rm SN}/{\rm day}) = 0.2289$.

3.2 Initial parameters for SN Ia progenitors

Figs 2-5 show the final outcomes of about 2400 binary evolution calculations in the initial orbital period–secondary mass ($\log P^{\rm i} - M_2^{\rm i}$) plane. The filled squares, circles and stars denote that the WD explodes as a SN Ia in the optically thick wind phase, in the stable H-shell burning phase and in the weak H-shell flash phase, respectively. The filled triangles represent that the WD explodes as a SN Ia, in which the accretion disk experiences instability. Some binaries fail to produce SNe Ia owing to nova explosions (which prevents the WD growing in mass; the open circles in these figures) or dynamically unstable mass-transfer (resulting in a common envelope; the crosses in these figures).

The contours of initial parameters for producing SNe Ia are also presented in these figures (solid curves are for the contours from the WD + MS channel, while dotted curves from the WD + RG channel). The left boundaries of the contours in these figures (solid lines; Figs 2-4 and panel (d) of Fig. 5) are set by the condition that RLOF starts when the donor star is on the ZAMS, while systems beyond the right boundary experience mass-transfer at a very high rate due to the rapid expansion of the donor stars in the Hertzsprung gap (HG) (solid lines) or RG stage (dotted lines) and they lose too much mass via the optically thick wind, preventing the WDs increasing their masses to the Ch mass. The upper boundaries are set mainly by a high mass-transfer rate owing to a large mass-ratio. The lower boundaries are constrained by the facts that the mass-transfer rate $\dot{M}_2$ should be high enough to ensure that the WD can grow in mass during outbursts and that the donor should be sufficiently massive for enough mass to be transferred onto the WD.

In Fig. 6, we overlay the contours for SN Ia production in the ($\log P^{\rm i}$, $M_2^{\rm i}$) plane for different initial WD masses. In panel (a), we give the contours of the WD + MS channel for producing SNe Ia with various WD masses (i.e. $M_{\rm WD}^{\rm i}$ = 0.61, 0.65, 0.7, 0.8, 0.9, 1.0, 1.1 and 1.2 $M_\odot$). Note that the enclosed region almost vanishes for $M_{\rm WD}^{\rm i} = 0.61\,M_\odot$, which is then assumed to be the minimum WD mass for producing SNe Ia from this channel. As a comparison, we also give the contours of the WD + RG channel in panel (b). If the initial parameters of a WD binary are located in the contours, a SN Ia is then assumed to be produced. Thus, these contours can be expediently used in BPS studies. The data points and the interpolation FORTRAN code for these contours can be supplied on request by contacting BW.

4 BINARY POPULATION SYNTHESIS

In order to investigate SN Ia birthrates and delay times for the WD + MS channel, we have performed a series of Monte

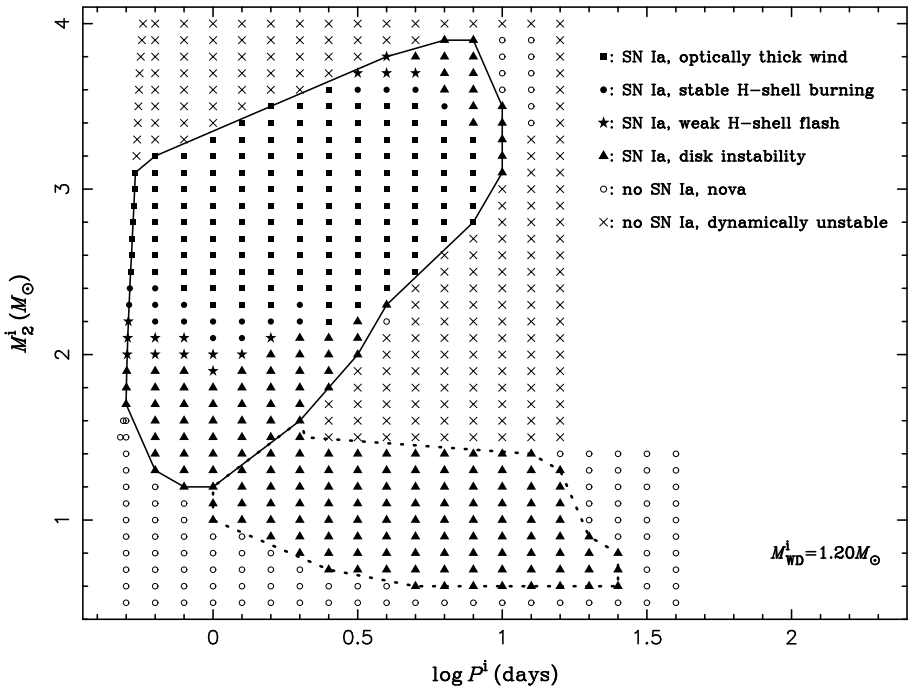

Figure 2. Final outcomes of the binary evolution calculations in the initial orbital period–secondary mass ($\log P^{\rm i}$, $M_2^{\rm i}$) plane of the CO WD + MS system for an initial WD mass of 1.2 $M_\odot$. Solid curves are for the contours from the WD + MS channel, while dotted curves from the WD + RG channel. The filled squares, circles and stars denote that the WD explodes as a SN Ia in the optically thick wind phase, in the stable H-shell burning phase and in the weak H-shell flash phase, respectively. The filled triangles represent that the WD explodes as a SN Ia, in which the accretion disk experiences instability. Open circles indicate systems that experience novae, preventing the WD from reaching 1.378 $M_\odot$, and crosses are those under dynamically unstable mass-transfer.

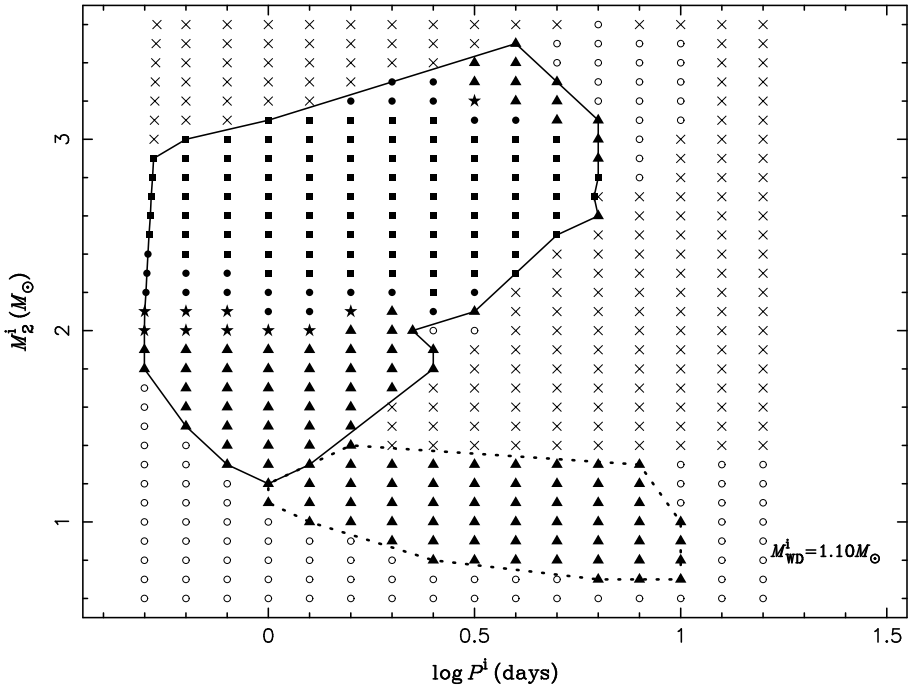

Figure 3. Similar to Fig. 2, but for an initial WD mass of 1.1 $M_\odot$.

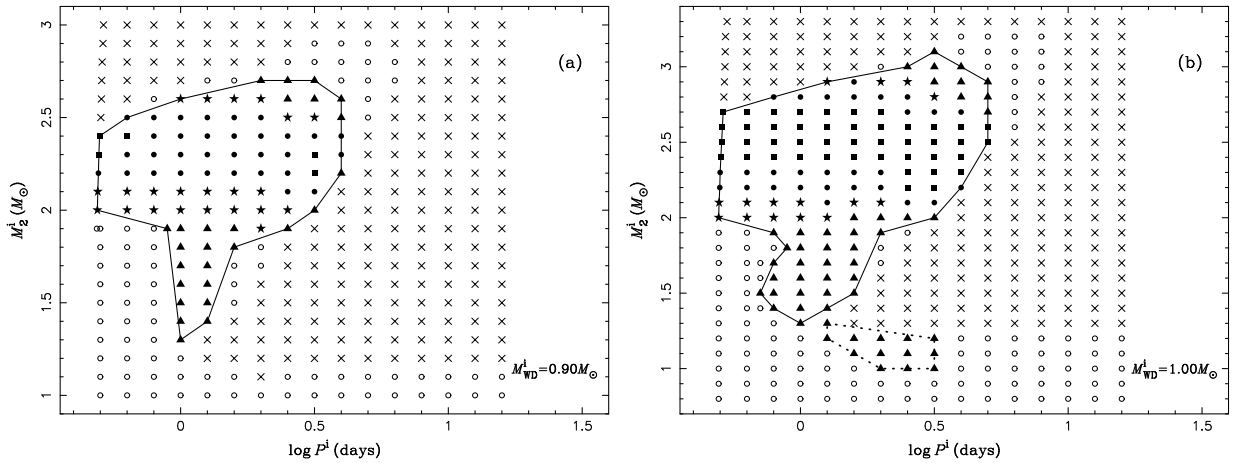

Figure 4. Similar to Fig. 2, but for initial WD masses of 0.9 and 1.0 $M_\odot$.

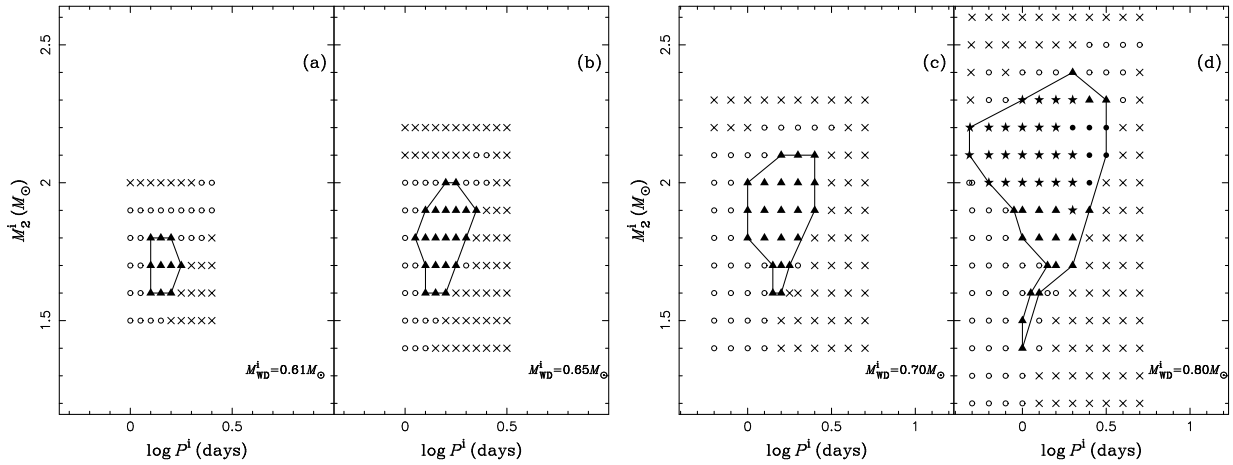

Figure 5. Similar to Fig. 2, but for initial WD masses of 0.61, 0.65, 0.7 and 0.8 $M_\odot$.

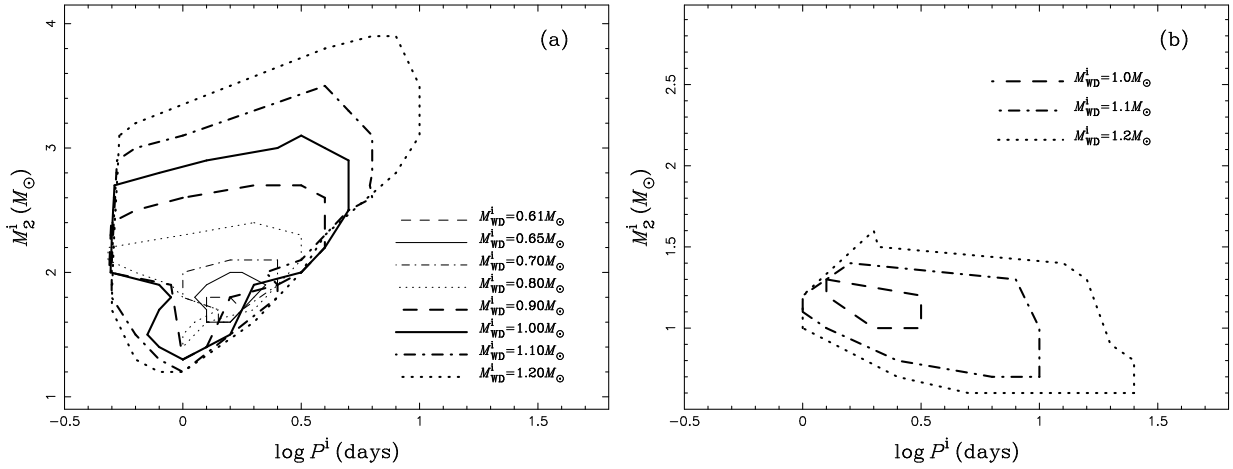

Figure 6. Panel (a): regions in the initial orbital period–secondary mass plane (log $P^{\rm i}$, $M_2^{\rm i}$) for the WD + MS channel that produce SNe Ia for initial WD masses of 0.61, 0.65, 0.7, 0.8, 0.9, 1.0, 1.1 and 1.2 $M_\odot$. The region almost vanishes for $M^{\rm i}_{\rm WD} = 0.61\,M_\odot$. Panel (b): similar to the panel (a), but the regions are for the WD + RG channel.

Carlo simulations in the BPS study. In each simulation, by using the Hurley's rapid binary evolution code (Hurley, Pols & Tout 2000, 2002), we have followed the evolution of 1×10^7 sample binaries from the star formation to the formation of the WD + MS systems according to three evolutionary channels (Sect. 4.2). We assumed that, if the parameters of a CO WD + MS system at the onset of the RLOF are located in the SN Ia production regions (panel (a) of Fig. 6), a SN Ia is produced. Note that, the method of the BPS study for the WD + RG channel is similar to that of the WD + MS channel.

4.1 Common envelope in binary evolution

In the SD model of SNe Ia, the progenitor of a SN Ia is a close WD binary system, which has most likely emerged from the common envelope (CE) evolution (Paczyński 1976) of a giant binary system. The CE ejection is still an open problem. Similar to the work of WCMH09, we also use the standard energy equations (Webbink 1984) to calculate the output of the CE phase. The CE is ejected if

$$\alpha_{\rm ce}\left(\frac{GM_{\rm don}^{\rm f}M_{\rm acc}}{2a_{\rm f}}-\frac{GM_{\rm don}^{\rm i}M_{\rm acc}}{2a_{\rm i}}\right)=\frac{GM_{\rm don}^{\rm i}M_{\rm env}}{\lambda R_{\rm don}}, \qquad (7)$$

where λ is a structure parameter that depends on the evolutionary stage of the donor, $M_{\rm don}$ is the mass of the donor, $M_{\rm acc}$ is the mass of the accretor, a is the orbital separation, $M_{\rm env}$ is the mass of the donor's envelope, $R_{\rm don}$ is the radius of the donor, and the indices i and f denote the initial and final values, respectively. The right side of the equation represents the binding energy of the CE, the left side shows the difference between the final and initial orbital energy, and $\alpha_{\rm ce}$ is the CE ejection efficiency, i.e. the fraction of the released orbital energy used to eject the CE. For this prescription of the CE ejection, there are two highly uncertain parameters (i.e. $\alpha_{\rm ce}$ and λ). As in previous studies, we combine $\alpha_{\rm ce}$ and λ into one free parameter $\alpha_{\rm ce}\lambda$, and set it to be 0.5 and 1.5 (e.g. WCMH09).

4.2 Evolutionary channels to WD + MS and WD + RG systems

According to the evolutionary phase of the primordial primary at the beginning of the first RLOF, there are three channels which can form CO WD + MS systems and then produce SNe Ia.

(1) *He star channel.* The primordial primary first fills its Roche lobe when it is in the HG (so-called early Case B mass-transfer defined by Kippenhahn & Weigert 1967). A CE may be formed when the lobe-filling star evolves to the RG stage owing to a large mass-ratio or a convective envelope of the mass donor star. After the CE ejection, the primary becomes a He star and continues to evolve. After the exhaustion of central He, the He star which now contains a CO-core may fill its Roche lobe again due to expansion of the He star itself, and transfer its remaining He-rich envelope to the MS companion star, eventually leading to the formation of a CO WD + MS system. For this channel, SN Ia explosions occur for the ranges $M_{1,\rm i}\sim4.0{-}7.0\,M_\odot$, $M_{2,\rm i}\sim1.0{-}2.0\,M_\odot$, and $P^{\rm i}\sim5{-}30$ days, where $M_{1,\rm i}$, $M_{2,\rm i}$ and $P^{\rm i}$ are the initial mass of the primary and the secondary at ZAMS, and the initial orbital period of a binary system.

(2) *EAGB channel.* If the primordial primary is on the early asymptotic giant branch (EAGB, i.e. He is exhausted in the centre of the star while thermal pulses have not yet started), a CE will be formed because of dynamically unstable mass-transfer. After the CE is ejected, the orbit decays and the primordial primary becomes a He RG. The He RG may fill its Roche lobe and start mass-transfer, which is likely stable and leaves a CO WD + MS system. For this channel, SN Ia explosions occur for the ranges $M_{1,\rm i}\sim2.5-6.5\,M_\odot$, $M_{2,\rm i}\sim1.5-3.0\,M_\odot$ and $P^{\rm i}\sim200-900$ days.

(3) *TPAGB channel.* The primordial primary fills its Roche lobe at the thermal pulsing asymptotic giant branch (TPAGB) stage. A CE is easily formed owing to dynamically unstable mass-transfer during the RLOF. After the CE ejection, the primordial primary becomes a CO WD, then a CO WD + MS system is produced. For this channel, SN Ia explosions occur for the ranges $M_{1,\rm i}\sim4.5{-}6.5\,M_\odot$, $M_{2,\rm i}\sim1.5{-}3.5\,M_\odot$, and $P^{\rm i}\gtrsim1000$ days.

Additionally, there is one channel which can form CO WD + RG systems and then produce SNe Ia (i.e. the *TPAGB channel* above). After a CO WD + MS system is produced via the *TPAGB channel*, the MS companion star continues to evolve until the RG stage, i.e. a CO WD + RG system is formed. For the CO WD + RG systems, SN Ia explosions occur for the ranges $M_{1,\rm i}\sim5.0{-}6.5\,M_\odot$, $M_{2,\rm i}\sim1.0{-}1.5\,M_\odot$, and $P^{\rm i}\gtrsim1500$ days.

4.3 Basic parameters for Monte Carlo simulations

In the BPS study, the Monte Carlo simulation requires as input the initial mass function (IMF) of the primary, the mass-ratio distribution, the distribution of initial orbital separations, the eccentricity distribution of binary orbit, and the star formation rate (SFR) (e.g. Han et al. 2002, 2003; Han, Podsiadlowski & Lynas-Gray 2007; WCMH09).

(1) The IMF of Miller & Scalo (1979) is adopted. The primordial primary is generated according to the formula of Eggleton, Tout & Fitechett (1989),

$$M_1^{\rm p}=\frac{0.19X}{(1-X)^{0.75}+0.032(1-X)^{0.25}}, \qquad (8)$$

where X is a random number uniformly distributed in the range [0, 1] and $M_1^{\rm p}$ is the mass of the primordial primary, which ranges from $0.1\,M_\odot$ to $100\,M_\odot$. The studies of the IMF by Kroupa, Tout & Gilmore (1993) and Zoccali et al. (2000) support this IMF.

(2) The initial mass-ratio distribution of the binaries, q', is quite uncertain for binary evolution. For simplicity, we take a constant mass-ratio distribution (Mazeh et al. 1992; Goldberg & Mazeh 1994),

$$n(q')=1, \qquad 0<q'\leqslant1, \qquad (9)$$

where $q'=M_2^{\rm p}/M_1^{\rm p}$. This constant mass-ratio distribution is supported by the study of Shatsky & Tokovinin (2002). As an alternative mass-ratio distribution we also consider uncorrelated binary components, i.e. both binary components are chosen randomly and independently from the same IMF (uncorrelated).

(3) We assume that all stars are members of binaries

Table 1. Galactic birthrates of SNe Ia for different simulation sets, where sets 1 and 4 are our standard models for the WD + MS and WD + RG channels, respectively.

Set	Channel	$\alpha_{\rm ce}\lambda$	$n(q')$	ν ($10^{-3}\,{\rm yr}^{-1}$)
1	WD + MS	0.5	Constant	1.793
2	WD + MS	1.5	Constant	1.415
3	WD + MS	0.5	Uncorrelated	0.275
4	WD + RG	0.5	Constant	0.028
5	WD + RG	1.5	Constant	0.026

and that the distribution of separations is constant in $\log a$ for wide binaries, where a is separation and falls off smoothly at small separation

$$a \cdot n(a) = \begin{cases} \alpha_{\rm sep}(a/a_0)^{\rm m}, & a \leqslant a_0, \\ \alpha_{\rm sep}, & a_0 < a < a_1, \end{cases} \quad (10)$$

where $\alpha_{\rm sep} \approx 0.07$, $a_0 = 10\,R_\odot$, $a_1 = 5.75\times10^6\,R_\odot = 0.13\,{\rm pc}$ and $m \approx 1.2$. This distribution implies that the numbers of wide binaries per logarithmic interval are equal, and that about 50 per cent of stellar systems have orbital periods less than 100 yr (Han, Podsiadlowski & Eggleton 1995).

(4) A circular orbit is assumed for all binaries. The orbits of semidetached binaries are generally circularized by the tidal force on a timescale which is much smaller than the nuclear timescale. Also, a binary is expected to become circularized during the RLOF.

(5) We simply assume a constant SFR over the last 15 Gyr or, alternatively, as a delta function, i.e. a single starburst. In the case of the constant SFR, we calibrate the SFR by assuming that one binary with a primary more massive than $0.8\,M_\odot$ is formed annually (see Iben & Tutukov 1984; Han, Podsiadlowski & Eggleton 1995; Hurley, Pols & Tout 2002). From this calibration, we can get SFR $= 5\,M_\odot{\rm yr}^{-1}$ (e.g. Willems & Kolb 2004), which successfully reproduces the ^{26}Al 1.809-MeV gamma-ray line and the core-collapse SN rate in the Galaxy (Timmes, Diehl & Hartmann 1997). It is obvious that for a galaxy with a different SFR the SN Ia rates will be scaled. For the case of the single starburst, we assume a burst producing $10^{11}\,M_\odot$ in stars, which is a typical mass of a galaxy. In fact, a galaxy may have a complicated star formation history. We only choose these two extremes for simplicity. A constant SFR is similar to the situation of spiral galaxies (Yungelson & Livio 1998; Han & Podsiadlowski 2004), while a delta function to that of elliptical galaxies or globular clusters.

5 THE RESULTS OF BINARY POPULATION SYNTHESIS

We performed five sets of simulations (see Table 1) with metallicity $Z = 0.02$ to systematically investigate Galactic birthrates of SNe Ia, where sets 1 and 4 are our standard models for the WD + MS and WD + RG channels, respectively, and with the best choice of model parameters (e.g. WCMH09). We vary the model parameters in the other sets to examine their influences on the final results.

In Fig. 7, we show the evolution of Galactic SN Ia birthrate by adopting $Z = 0.02$ and SFR $= 5\,M_\odot{\rm yr}^{-1}$ both for the WD + MS channel (thick curves) and the WD + RG channel (thin curves). The simulation for the WD + MS channel gives Galactic SN Ia birthrate of $\sim1.8\times10^{-3}$ yr^{-1} according to our standard model (set 1). The result is higher by a factor of 2−3 than previous studies by Han & Podsiadlowski (2004, HP04) ($\sim0.6-0.8\times10^{-3}$ yr^{-1}). This is mainly attributed to the effect of the accretion disk instability, which can increase the accretion rate onto the WD during outbursts, leading to higher effective WD growth rates and a larger fraction of systems becoming SN Ia progenitors. However, the result from this work is still lower than that inferred observationally (i.e. $3-4\times10^{-3}$ yr^{-1}: van den Bergh & Tammann 1991; Cappellaro & Turatto 1997). The simulation for a constant mass-ratio distribution with $\alpha_{\rm ce}\lambda = 1.5$ (set 2) gives SN Ia birthrate of $\sim1.4\times10^{-3}$ yr^{-1}, which is lower than the case of $\alpha_{\rm ce}\lambda = 0.5$ (the binaries resulted from the CE ejections tend to have slightly closer orbits for $\alpha_{\rm ce}\lambda = 0.5$ and are more likely to locate in the SN Ia production region). If we adopt a mass-ratio distribution with uncorrelated binary components and $\alpha_{\rm ce}\lambda = 0.5$ (set 3), the SN Ia birthrate from the WD + MS channel will be lower by an order of magnitude (see dotted curve in Fig.7). This is because most of the donors in the WD + MS channel are not very massive which has the consequence that WDs cannot accrete enough mass to reach the Ch mass. Similar to previous studies (e.g. Yungelson & Livio 1998; HP04), the Galactic SN Ia birthrate from the WD + RG channel is still low ($\sim3\times10^{-5}$ yr^{-1}). The studies in this paper imply that the WD + MS and WD + RG channels are only subclasses of SN Ia production, and there may be some other channels or mechanisms also contributing to SNe Ia, e.g. WD + He star channel or double-degenerate channel. Especially, as mentioned by WCMH09, the WD + He star channel can give a Galactic birthrate of $\sim0.3\times10^{-3}$ yr^{-1}, and is considered to be an important channel to produce SNe Ia with short delay times. The SN Ia birthrates shown in this figure seem to be so completely flat after the first rise, for the specific reason see Sect. 3 of WCMH09.

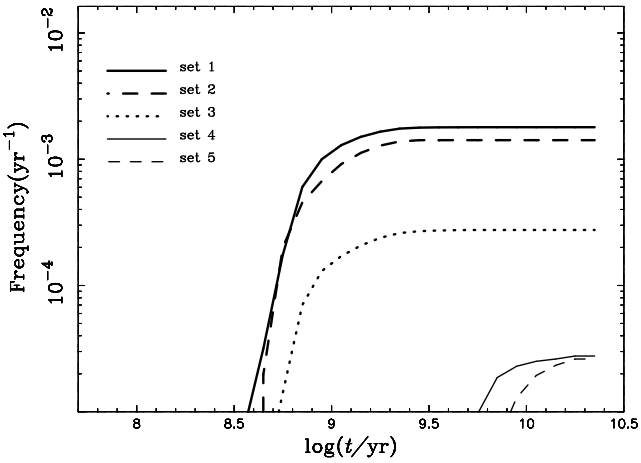

Figure 7. Evolution of Galactic birthrates of SNe Ia for a constant star formation rate ($Z = 0.02$, SFR $= 5\,M_\odot{\rm yr}^{-1}$). The key to the line-styles representing different sets is given in the upper left corner.

Fig. 8 displays the evolution of SN Ia birthrates for a single starburst with a total mass of $10^{11}\,M_\odot$. In the figure we see that SNe Ia from the WD + MS channel (thick curves) have the delay times of $\sim$250 Myr−6.3 Gyr (while

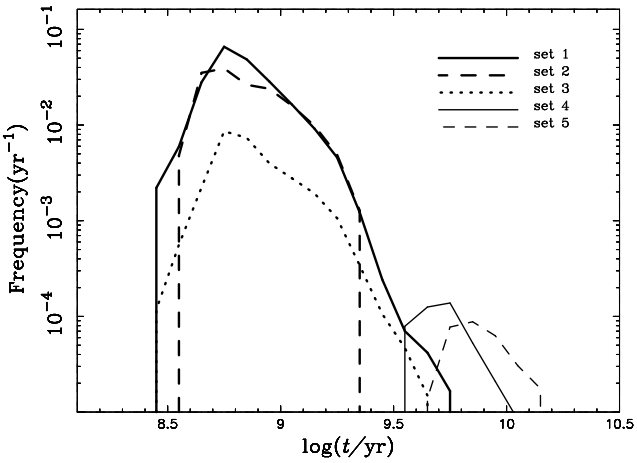

Figure 8. Similar to Fig. 7, but for a single starburst with a total mass of $10^{11}\,M_{\odot}$.

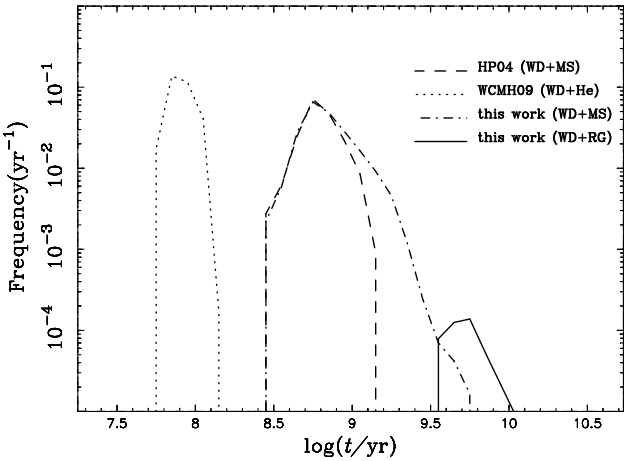

Figure 9. Same as Fig. 8, but for different SD models. The SD models are from HP04 (dashed curve), WCMH09 (dotted curve) and this work (dot-dashed curve is for the WD + MS channel, while solid curve is for the WD + RG channel). All curves are for a constant mass-ratio distribution and with $\alpha_{\rm ce}\lambda = 0.5$.

SNe Ia from the WD + RG channel have the delay times of $\gtrsim$3 Gyr; thin curves). This figure also shows that a high value of $\alpha_{\rm ce}\lambda$ leads to a systematically later explosion time for these two channels (e.g. the cases of $\alpha_{\rm ce}\lambda = 0.5$ and 1.5 for a constant mass-ratio distribution). This is because a high value of $\alpha_{\rm ce}\lambda$ leads to wider WD binaries, and, as a consequence, it takes a longer time for the companion to evolve to fill its Roche lobe.

In Fig. 9, we compare the theoretical delay time distributions (DTDs) of SNe Ia for different SD models. The SD models are from HP04 (dashed curve), WCMH09 (dotted curve) and this work (dot-dashed curve is for the WD + MS channel, while solid curve is for the WD + RG channel). In this figure, the WD + MS channel of HP04 may contribute to the SNe Ia with intermediate delay times (100 Myr−1 Gyr: for a detailed discussion see Schawinski 2009). The results of the WD + He star channel from WCMH09 may provide a possible ways to explain the SNe Ia with short delay times ($\lesssim$100 Myr). In addition, for SNe Ia with the long delay times ($\gtrsim$1 Gyr), about one third of SNe Ia from the WD + MS channel (dot-dashed curve) and all SNe Ia from the WD + RG channel (solid curve) can contribute to the old populations of SN Ia progenitors. Note, Chen & Li (2007) studied the WD + MS channel by considering a circumbinary disk which extracts the orbital angular momentum from the binary through tidal torques. The study can also provide a possible ways of producing such old SNe Ia ($\sim$1−3 Gyr). Finally, we emphasize that SNe Ia may be from several different progenitor systems.

6 DISCUSSION

The regions (Fig. 6 in this paper) for producing SNe Ia depend on many uncertain input parameters, in particular for the duty cycle which is poorly known. The main uncertainties lie in the facts that it varies from one binary system to another and may evolve with the orbital periods and mass-transfer rates (e.g. Lasota 2001; Xu & Li 2009). This is the reason why we choose an intermediate value (0.01) rather than other extreme ones (e.g. 0.1 or 10^{-3}). However, we also did some tests for a higher or lower value of the duty cycle. We find that the variation of the duty cycle value will influence the regions for producing SNe Ia, especially for the WD + RG channel (for a high value (0.1), the regions will be shifted to higher period; for a low value (10^{-3}), the regions will be shifted to lower period). For these two extreme duty cycle values, the SN Ia birthrate from the WD + RG channel will be lower due to the smaller regions for producing SNe Ia.

In our binary evolution calculations we have not considered the influence of rotation on the H-accreting WDs. The calculations of Yoon, Langer & Scheithauer (2004) showed that the He-shell burning is much less violent when rotation is taken into account. This may significantly increase the He-accretion efficiency ($\eta_{\rm He}$ in this paper). Meanwhile, the maximum stable mass of a rotating WD may be above the standard Ch mass (i.e. the super-Ch mass model: Uenishi, Nomoto & Hachisu 2003; Yoon & Langer 2005; Chen & Li 2009). However, we mainly focus on the standard Ch mass explosions of the accreting WDs in this work.

In our BPS studies we assume that all stars are in binaries and about 50 per cent of stellar systems have orbital periods less than 100 yr. In fact, this is known to be a simplification, and the binary fractions may depend on metallicity, environment, spectral type, etc. If we adopt 40 per cent of stellar systems have orbital periods below 100 yr by adjusting the parameters in Equation (10), we estimate that the Galactic SN Ia birthrate from the WD + MS channel will decrease to be $\sim 1.4\times10^{-3}$ yr^{-1} according to our standard model (the birthrate from the WD + RG channel will decrease to be $\sim 2\times10^{-5}$ yr^{-1}). In addition, Umeda et al. (1999) concluded that the upper limit mass of CO cores born in binaries is about $1.07\,M_{\odot}$. If this value is adopted as the upper limit of the CO WD, the SN Ia birthrate from the WD + MS channel will decrease to be $\sim 1.7\times10^{-3}$ yr^{-1} (the birthrate from the WD + RG channel will decrease to be $\sim 1\times10^{-5}$ yr^{-1}).

The Galactic SN Ia birthrate from the WD + RG channel is $\sim 3\times10^{-5}$ yr^{-1} according to our standard model, which is low compared with observations, i.e. SNe Ia from this channel may be rare. However, further study on this chan-

nel is necessary, since this channel may explain some SNe Ia with long delay times. In addition, it is suggested that, RS Oph and T CrB, both recurrent novae are probable SN Ia progenitors and belong to the WD + RG channel (e.g. Belczyński & Mikolajewska 1998; Hachisu, Kato & Nomoto 1999b; Sokoloski et al. 2006; Hachisu, Kato & Luna 2007). Meanwhile, by detecting Na I absorption lines with low expansion velocities, Patat et al. (2007) suggested that the companion of the progenitor of SN 2006X may be an early RG star. Additionally, Voss & Nelemans (2008) studied the pre-explosion archival X-ray images at the position of the recent SN 2007on, and they considered that its progenitor may be a WD + RG system.

7 SUMMARY

Employing Eggleton's stellar evolution code with the prescription of Hachisu et al. (1999a) for the mass-accretion of CO WDs, and including the effect of the instability of accretion disk on the evolution of WD binaries, we performed binary evolution calculations for about 2400 close WD binaries. The calculated results further confirm that the disk instability could substantially increase the mass-accumulation efficiency for accreting WDs, and cause the possible SNe Ia to occur in systems with $\lesssim 2\,M_{\odot}$ donor stars (see also King, Rolfe & Schenker 2003; Xu & Li 2009). We find that the Galactic SN Ia birthrate from the WD + MS channel is $\sim 1.8 \times 10^{-3}$ yr^{-1} according to our standard model, which is higher than previous results. However, similar to previous studies, the birthrate from the WD + RG channel is still low ($\sim 3 \times 10^{-5}$ yr^{-1}). We also find that about one third of SNe Ia from the WD + MS channel and all SNe Ia from the WD + RG channel can contribute to the old populations ($\gtrsim$1 Gyr) of SN Ia progenitors. The companion stars of SNe Ia with long delay times in this work would survive in the SN explosion and show distinguishing properties. In future investigations, we will explore the properties of the companion stars after SN explosion, which could be verified by future observations.

ACKNOWLEDGMENTS

We thank an anonymous referee for his/her valuable comments that helped to improve the paper. This work is supported by the National Natural Science Foundation of China (Grant Nos. 10873008 and 10821061), the National Basic Research Program of China (Grant Nos. 2007CB815406 and 2009CB824800), and the Yunnan Natural Science Foundation (Grant No. 08YJ041001).

REFERENCES

Alexander D. R., Ferguson J. W., 1994, ApJ, 437, 879
Andronov N., Pinsonneault M., Sills A., 2003, ApJ, 582, 358
Aubourg E., Tojeiro R., Jimenez R., Heavens A. F., Strauss M. A., Spergel D. N., 2008, A&A, 492, 631
Belczyński K., Mikolajewska J., 1998, MNRAS, 296, 77
Botticella M. T. et al., 2008, A&A, 479, 49
Cappellaro E., Turatto M., 1997, in Ruiz-Lapuente P., Cannal R., Isern J., eds, Thermonuclear Supernovae. Kluwer, Dordrecht, P. 77
Chen W.-C., Li X.-D., 2007, ApJ, 658, L51
Chen W.-C., Li X.-D., 2009, ApJ, 702, 686
Chen X., Tout C. A., 2007, Chin. J. Astro. Astrophys., 7, 245
Eggleton P. P., 1971, MNRAS, 151, 351
Eggleton P. P., 1972, MNRAS, 156, 361
Eggleton P. P., 1973, MNRAS, 163, 279
Eggleton P. P., Tout C. A., Fitechett M. J., 1989, ApJ, 347, 998
Fedorova A. V., Tutukov A. V., Yungelson L. R., 2004, Astron. Lett., 30, 73
Goldberg D., Mazeh T., 1994, A&A, 282, 801
Greggio L., Renzini A., 1983, A&A, 118, 217
Hachisu I., Kato M., Luna G. J. M., 2007, ApJ, 659, L153
Hachisu I., Kato M., Nomoto K., 1996, ApJ, 470, L97
Hachisu I., Kato M., Nomoto K., Umeda H., 1999a, ApJ, 519, 314
Hachisu I., Kato M., Nomoto K., 1999b, ApJ, 522, 487
Han Z., 1998, MNRAS, 296, 1019
Han Z., 2008, ApJ, 677, L109
Han Z., Podsiadlowski Ph., 2004, MNRAS, 350, 1301 (HP04)
Han Z., Podsiadlowski Ph., 2006, MNRAS, 368, 1095
Han Z., Podsiadlowski Ph., Eggleton P. P., 1994, MNRAS, 270, 121
Han Z., Podsiadlowski Ph., Eggleton P. P., 1995, MNRAS, 272, 800
Han Z., Podsiadlowski Ph., Lynas-Gray A. E., 2007, MNRAS, 380, 1098
Han Z., Podsiadlowski Ph., Maxted P. F. L., Marsh T. R., 2003, MNRAS, 341, 669
Han Z., Podsiadlowski Ph., Maxted P. F. L., Marsh T. R., Ivanova N., 2002, MNRAS, 336, 449
Han Z., Tout C. A., Eggleton P. P., 2000, MNRAS, 319, 215
Hansen B. M. S., 2003, ApJ, 582, 915
Hillebrandt W., Niemeyer J. C., 2000, ARA&A, 38, 191
Hurley J. R., Pols O. R., Tout C. A., 2000, MNRAS, 315, 543
Hurley J. R., Pols O. R., Tout C. A., 2002, MNRAS, 329, 897
Iben I. Jr., Tutukov A. V., 1984, ApJS, 54, 335
Iglesias C. A., Rogers F. J., 1996, ApJ, 464, 943
Justham S., Wolf C., Podsiadlowski P., Han Z., 2009, A&A, 493, 1081
Kato M., Hachisu I., 2004, ApJ, 613, L129
King A. R., Frank J., Kolb U., Ritter H., 1997, ApJ, 484, 844
King A. R., Rolfe D. J., Schenker K., 2003, MNRAS, 341, L35
Kippenhahn R., Weigert A., 1967, Z. Ap., 65, 251
Krishnamurthi A., Pinsonneault M. H., Barnes S., Sofia S., 1997, ApJ, 480, 303
Kroupa P., Tout C. A., Gilmore G., 1993, MNRAS, 262, 545
Langer N., Deutschmann A., Wellstein S., Höflich P., 2000, A&A, 362, 1046
Lasota J.-P., 2001, New Astro. Rev., 45, 449
Li X.-D., van den Heuvel E. P. J., 1997, A&A, 322, L9

Li X.-D., Wang Z.-R., 1998, ApJ, 500, 935
Lü G., Zhu C., Wang Z., Wang N., 2009, MNRAS, 396, 1086
Mannucci F., Della Valle M., Panagia N., 2006, MNRAS, 370, 773
Matteucci F., Greggio L., 1986, A&A, 154, 279
Mazeh T., Goldberg D., Duquennoy A., Mayor M., 1992, ApJ, 401, 265
Meng X., Chen X., Han Z., 2009, MNRAS, 395, 2103
Miller G. E., Scalo J. M., 1979, ApJS, 41, 513
Nomoto K., Iben I., 1985, ApJ, 297, 531
Nomoto K., Iwamoto K., Kishimoto N., 1997, Sci, 276, 1378
Nomoto K., Thielemann F-K., Yokoi K., 1984, ApJ, 286, 644
Osaki Y., 1996, PASP, 108, 39
Paczyński B., 1976, in Eggleton P. P., Mitton S., Whelan J., eds. Structure and Evolution of Close Binaries. Kluwer, Dordrecht, p. 75
Patat F. et al., 2007, Sci, 317, 924
Perlmutter S. et al., 1999, ApJ, 517, 565
Podsiadlowski Ph., Mazzali P., Lesaffre P., Han Z., Förster F., 2008, New Astro. Rev., 52, 381
Podsiadlowski Ph., Rappaport S., Pfahl E. D., 2002, ApJ, 565, 1107
Pols O. R., Schröder K. P., Hurly J. R., Tout C. A., Eggleton P. P., 1998, MNRAS, 298, 525
Pols O. R., Tout C. A., Eggleton P. P., Han Z., 1995, MNRAS, 274, 964
Pols O. R., Tout C. A., Schröder K. P., Eggleton P. P., Manners J., 1997, MNRAS, 289, 869
Riess A. et al., 1998, AJ, 116, 1009
Röpke F. K., Hillebrandt W., 2005, A&A, 431, 635
Ruiter A. J., Belczynski K., Fryer C. L., 2009, ApJ, 699, 2026
Ruiz-Lapuente P. et al., 2004, Nat, 431, 1069
Saio H., Nomoto K., 1985, A&A, 150, L21
Schawinski K., 2009, MNRAS, 397, 717
Schröder K. P., Pols O. R., Eggleton P. P., 1997, MNRAS, 285, 696
Shatsky N., Tokovinin A., 2002, A&A, 382, 92
Sills A., Pinsonneault M. H., Terndrup D. M., 2000, ApJ, 534, 335
Smak J., 1983, ApJ, 272, 234
Sokoloski J. L., Luna G. J. M., Mukai K., Kenyon S. J., 2006, Nat, 442, 276
Timmes F. X., Diehl R., Hartmann D. H., 1997, ApJ, 479, 760
Timmes F. X., Woosley S. E., Taam R. E., 1994, ApJ, 420, 348
Totani T., Morokuma T., Oda T., Doi M., Yasuda N., 2008, PASJ, 60, 1327
Uenishi T., Nomoto K., Hachisu I., 2003, ApJ, 595, 1094
Umeda H., Nomoto K., Yamaoka H., Wanajo S., 1999, ApJ, 513, 861
van den Bergh S., Tammann G. A., 1991, ARA&A, 29, 363
van Paradijs J., 1996, ApJ, 464, L139
Voss R., Nelemans G., 2008, Nat, 451, 802
Wang B., Meng X., Chen X., Han Z., 2009a, MNRAS, 395, 847
Wang B., Chen X., Meng X., Han Z., 2009b, ApJ, 701, 1540 (WCMH09)
Wang B., Meng X., Wang X.-F., Han Z., 2008a, Chin. J. Astro. Astrophys., 8, 71
Wang X.-F. et al., 2008b, ApJ, 675, 626
Warner B., 1995, Cataclysmic Variable Stars. Cambridge, England: Cambridge University Press
Webbink R. F., 1984, ApJ, 277, 355
Whelan J., Iben I., 1973, ApJ, 186, 1007
Willems B., Kolb U., 2004, A&A, 419, 1057
Xu X.-J., Li X.-D., 2009, A&A, 495, 243
Yoon S.-C., Langer N., 2005, A&A, 435, 967
Yoon S.-C., Langer N., Scheithauer S., 2004, A&A, 425, 217
Yungelson L., Livio M., 1998, ApJ, 497, 168
Zoccali M., Cassisi S., Frogel J. A., Gould A., Ortolani S., Renzini A., Rich R. M., Stephens A. W., 2000, ApJ, 530, 418